Carbon-13 Kinetic Isotope Effects in the Catalytic Oxidation of CO over Ag

Ivan Kobal,[†] Uwe Burghaus,[‡] Marjan Senegačnik,[†] and Nives Ogrinc*[,†]

J. Stefan Institute, Jamova 39, P.O. Box 3000, 1001 Ljubljana, Slovenia, and Centro di Fisica, via Dodecaneso 33, 16146 Genova, Italy

Received: February 11, 1998; In Final Form: June 16, 1998

The ^{13}C kinetic isotope effects in the catalytic oxidation of carbon monoxide over silver wool were found in the temperature range 343−453 K with the following temperature dependence: $100 \ln(k_{12}/k_{13}) = (3.398 - 630/T) \pm 0.083$. A reaction CO/O_2 gas mixture of 1:2 ratio was used in a static system with initial pressures ranging from 20 to 40 kPa. Under these conditions the reaction obeys the rate law $dP_{CO}/dt = -k_1 P_{CO}$ and has an apparent activation energy of 59.3 ± 1.7 kJ mol^{-1}. In our theoretical interpretation, based on Bigeleisen's formalism, various geometries of $(CO_2)^{\ddagger}$ were applied as transition states of the rate determining step, and only a $(CO_2)^{\ddagger}$ with an interbond angle of 110° and stretching force constants of 1700 and 1000−1400 N m^{-1} could explain the experimental results.

Introduction

Carbon monoxide oxidation catalyzed by transition metal surfaces was one of the first reactions studied by surface science methods.[1] Since that time carbon monoxide oxidation has served as the most important and best understood model for bimolecular surface reactions.[2] Nearly all methods and techniques available for both experimental[2] and theoretical[3] studies have been applied. Additionally, CO oxidation is important for technical applications, such as the three-way catalyst used for cleaning of exhaust pollution,[4] and it has been used to improve the performance of special laser light sources (e.g., closed-cycle CO_2 lasers[5]). Although a large number of studies have been conducted on single-crystal surfaces,[2,6−8] relatively few publications[9] deal with CO oxidation under measuring conditions that might be relevant for technical applications.

Despite a controversy about the Ag(111) surface[10] it is well accepted that oxygen adsorbs molecularly on all silver single-crystal surfaces for adsorption temperatures below about $T_s = 150$ K, whereas dissociative adsorption takes place in the temperature range most important for technical applications, i.e., $T_s > \sim 150$ K.[6,7] This is also expected for the silver wool used in our work. Additionally, the occupation of subsurface sites has frequently been reported. On the other hand, above about $T_s = 100$ K the low heat of adsorption of CO leads, even on nonclosed packed silver surfaces, to negligible CO coverages.[11]

Investigations of the CO_2 formation were mainly focused on the oxidation reaction by atomically bonded oxygen, thereby presenting evidence that the reaction had to be explained over the whole reaction temperature range by the Langmuir−Hinshelwood mechanism. Most likely the local onset of an oxygen-induced surface reconstruction leads to very complicated kinetics for the Ag(110) surface, which could be modeled by assuming kinetically distinct atomic oxygen species.[6]

Remarkably, the reaction by atomically adsorbed oxygen already takes place with high yields at $T_s = 100$ K. The CO oxidation above $T_s = 300$ K on Ag(110) is dominated by a self-accelerating CO_2 formation that is related to the relief of the surface reconstruction[7] rather than to diffusion-limited reaction kinetics.[8] For more close-packed surfaces of silver the influence of impurities on the oxidation kinetics as well as much smaller rates for CO_2 formation as compared to Ag(110) have been reported.[12] To the best of our knowledge the influence of subsurface oxygen on the kinetics of CO_2 formation has not yet been systematically investigated on silver surfaces. With respect to the oxidation reaction by molecularly adsorbed oxygen, silver surfaces showed unique kinetics. On palladium and platinum surfaces, for example, the CO_2 formation could till now only be observed by a thermally or photon induced interatomic bond breaking of adsorbed oxygen molecules.[13] For Ag(110) and Ag(100), however, the CO oxidation by molecularly adsorbed oxygen could be observed with adsorbed oxygen molecules directly involved in the primary reaction steps ("chemically" induced bond breaking).[14] Note, however, that preliminary results on gold surfaces also show evidence for a reaction pathway of CO_2 formation related to adsorbed oxygen molecules.[15]

Despite of a large number of studies focused on the kinetics and the adsorption of the participating reactants,[2,8] little work has been conducted with respect to an identification of the geometry of a possible transition state for CO_2 formation. Carbon monoxide adsorbed most likely upright[12] also on silver surfaces and the CO_2 molecule is of linear geometry. Thus, a large change of the bond angle during the formation of CO_2 must take place. Geometries for the $(CO_2)^{\ddagger}$ transition state such as flat adsorbed CO_2 molecules,[16] intermediates with an interbond angle of 120°,[17] and upright adsorbed CO_2 have been suggested rather speculatively.[18] The possible geometry for the $(CO_2)^{\ddagger}$ complex remains still unclear for a number of transitition metal surfaces. Carbonate formation is not expected here and a $(CO_3)^{\ddagger}$ transition state may thus be ruled out.

The aim of this work was to apply the kinetic isotope effect (KIE) in order to elucidate the reaction rates and the mechanism for a technically relevant silver catalyst as well as to investigate possible geometries of the rate-determining transition states. This approach has been applied for a long time and can still, in addition to other methods, be successfully used in providing

[†] J. Stefan Institute.
[‡] Centro di Fisica.

S1089-5647(98)01051-7 CCC: $15.00
Published on Web 08/11/1998

additional information about the kinetics and mechanism of a number of reactions.[19−25]

2. Experimental Section

A. Reaction System and Method. The ratio of the rate constants, k_{12}/k_{13}, for CO oxidation catalyzed by silver is defined by the overall chemical equations

$$^{12}C^{16}O + {}^{1}/_{2}\,{}^{16}O_2 \xrightarrow{k_{12}} {}^{12}C^{16}O_2$$

$$^{13}C^{16}O + {}^{1}/_{2}\,{}^{16}O_2 \xrightarrow{k_{13}} {}^{13}C^{16}O_2$$

The reaction was investigated in the temperature range 343−453 K by using carbon monoxide and oxygen of natural isotopic abundance. The kinetic isotope effects, k_{12}/k_{13}, were determined by the traditional isotopic competative technique of analyzing the product after a known extent of reaction. The values of the ratio of the isotopic rate constants were calculated by the equation[26,27]

$$\frac{k_{12}}{k_{13}} = \frac{\ln(1-f)}{\ln(1-fS(\,{}^{13}_{12}))} \qquad (1)$$

where f denotes the extent of reaction defined by $f = P_{CO_2}/P^0_{CO}$ with P^0_{CO} initial CO pressure and P_{CO_2} the pressure of CO_2 formed and the enrichment factor $S(\,{}^{13}_{12}) = R_f/R_1$ where R_f, R_1 are the $^{13}C^{16}O_2/^{12}C^{16}O_2$ isotopic ratios in the carbon dioxide at the extent of reaction f and at $f = 1$, i.e., after a complete CO conversion.

B. Materials. *Gases*. Both the carbon monoxide and oxygen used were of natural isotopic composition. The carbon monoxide (L′Air Liquide, France) had a purity of 99.9% and was used without further purification. The impurities may affect reaction rates, but because we are dealing with a ratio of the rate constants we assume this effect is canceled out. The oxygen from a commercial cylinder was purified by distillation at liquid nitrogen temperature. As checked by a mass spectrometer, the impurity level was below 0.2% with nitrogen as the main impurity. The reaction gas mixture was obtained by mixing the carbon monoxide and oxygen in the molar ratio 1:2. Hydrogen used for the silver catalyst treatment was commercially available high purity grade gas (99.9%, GTW, Munich, Germany). It was used without further purification.

Catalyst. The reagent grade silver wool, supplied by BDH Chemicals, was used as the catalyst. It was reported to contain not less than 99.99% of silver after degreasing and had an apparent geometrical area of 135 $cm^2\ g^{-1}$. A single 3 g sample of catalyst was used for all of the preliminary and subsequent kinetic and KIE determination runs at 343 and 373 K. However, experiments at 413 and 453 K were conducted with a 0.12 g portion of the catalyst. Prior to measurements the silver wool was degreased by refluxing under benzene for 16 h and, additionally, the following pretreatment has been used. The pretreatment, performed in the reaction vessel at 773 K, comprised a reduction with hydrogen (30 kPa) for 3 h followed by outgassing for 2 h at a residual pressure of 10 mPa. To ensure its reproducible operation the catalyst was conditioned by first catalyzing 10 oxidation runs in the temperature range 523−573 K and then 10 runs at 373 K. Between measurements the catalyst was outgassed at 737 K for 30 min to a residual pressure of 10 mPa. A few of these runs were preceeded by catalyst pretreatment with hydrogen (30 kPa) at 737 K.

C. Apparatus. All the experiments were carried out in a Pyrex glass vacuum system described elsewhere.[28,29] Its main parts are a 10 dm^3 vessels for storing CO, oxygen, and CO/O_2 mixtures, traps for purification of CO_2, a mercury manometer, a Toepler mercury pump, and a 220 cm^3 cylindrical quartz reaction vessel (ϕ 40 mm). The desired reaction temperature was provided by an electric tube furnace and controlled within ±1 K by means of a thermoregulator connected with a NiCr−Ni thermocouple attached to the outer surface of the reaction vessel.

D. Procedure. *KIE Determinations.* The measurements of the ratio of isotopic rate constants, k_{12}/k_{13}, were carried out at four reaction temperatures: 343, 373, 413, and 443 K. The standard procedure was to admit a known pressure (20−40 kPa) of starting $CO-O_2$ mixture ($CO:O_2 = 1:2$) into the evacuated reaction vessel, maintained at the temperature of the following reaction. After allowing the oxidation to proceed for a predetermined time, required for 20−50% conversion, it was stopped by removing the furnace and cooling the vessel to room temperature. The CO_2 formed was then frozen out by circulating the reaction mixture through the liquid nitrogen trap. Following the evacuation of residual CO and O_2, CO_2 was purified by twice sublimating at 351 K. To improve the accuracy of determination of the extent of reaction f, the CO_2 pressure was measured in the calibrated bulb having $\sim{}^{1}/_{10}$ of the volume of the reaction vessel.

For isotopic analysis, a double collector mass spectrometer was used. Carbon dioxide formed up to the extent of reaction, f, was analyzed to get R_f in eq 1, and carbon dioxide obtained by a complete conversion of CO to CO_2, $f = 1$, was analyzed to get R_1. CO_2 thus obtained has the same isotopic composition as the original CO.

Kinetic Runs. For the kinetic study the total pressure of reaction mixture as a function of the reaction time was detected in the reaction vessel by a mercury U-tube manometer. In most of the runs the kinetics up to 90% of conversion were observed. Because of the reaction stoichiometry the partial CO, CO_2, and O_2 pressures can be evaluated from measured total pressures by

$$P_{CO} = 2(P_t - P_\infty)$$

$$P_{CO_2} = 2(P_0 - P_t)$$

$$P_{O_2} = P_t - 2(P_0 - P_\infty)$$

with P_0, P_t, and P_∞ being the total pressures at reaction times 0, t, and ∞, i.e., after the complete CO converson.

3. Results

Kinetic Isotope Effects. The experimental conditions and values of kinetic isotopic effects are given in Table 1, using the symbols as defined above (see eq 1). The ^{13}C kinetic isotope effects are normal in the sense that $k_{12} > k_{13}$, but they clearly exhibit an anomalous temperature dependence by increasing with increasing reaction temperature. An Arrhenius plot of $\ln(k_{12}/k_{13})$ vs $1/T$ yields the relation

$$100\ (\ln k_{12}/k_{13}) = \left(3.398 - \frac{630}{T}\right) \pm 0.083$$

The isotopic fractionation eq 1, used for the evaluation of experimental kinetic isotope effects, applies in the tracer case to any overall reaction of arbitrary mechanism, provided it is irreversible. To get the relevant information, the oxidation runs with a natural $CO-O_2$ mixture were conducted at 373 K in the

TABLE 1: ^{13}C Kinetic Isotope Effects in the Silver-Catalyzed Carbon Monoxide Oxidation[a]

temp, K	catalyst mass, g	f	$S(^{13}_{12})$	k_{12}/k_{13}
343	3	0.1865	0.9865	1.0152
		0.1948	0.9858	1.0161
		0.2007	0.9861	1.0158
		0.2609	0.9868	1.0156
373	3	0.3081	0.9853	1.0180
		0.2434	0.9853	1.0172
		0.2116	0.9858	1.0163
		0.2827	0.9858	1.0171
		0.2333	0.9857	1.0166
		0.1826	0.9844	1.0176
		0.2236	0.9846	1.0178
		0.2230	0.9844	1.018
413	0.12	0.1491	0.9811	1.0209
		0.0617	0.9841	1.0167
		0.1671	0.9831	1.0189
		0.1901	0.9833	1.0189
		0.1816	0.9831	1.0190
		0.1132	0.9827	1.0187
453	0.12	0.1587	0.9828	1.0191
		0.2941	0.9837	1.0198
		0.2288	0.9822	1.0207
		0.1924	0.9819	1.0205
		0.1878	0.9813	1.0212

[a] Experimental errors: for temperature, ±1 K; for catalyst mass, ±10 mg; for f, ±0.005; for S, ± 0.0002.

presence of added $^{14}CO_2$. The activity of $^{14}CO_2$ used was such that less than 0.01% could easily be detected by means of an ionization chamber connected to a vibrating reed electrometer. Prior to the radiocarbon assay, the separated CO was purged twice by freezing out equal amounts of added natural CO_2 and then oxidizing to CO_2. No activity larger than the background activity could be detected. This fact indicates that under reaction conditions used in KIE determinations neither the reverse reaction nor the carbon isotopic exchange between CO and CO_2 occur significantly.

Kinetics. The principle objectives of the performed kinetic investigations were the determination of the rate law and the activation energy of the reaction for the same conditions as used for our measurement of ^{13}C kinetic isotope effects. Based on the experience, gained by prior studies of other groups and our own investigations, only the following two rate laws were checked

$$\frac{dP_{CO}}{dt} = -k_1 P_{CO} \tag{2}$$

and

$$\frac{dP_{CO}}{dt} = -k_2 \frac{P_{CO}}{P_{CO_2}} \tag{3}$$

with k denoting the respective overall rate constant. After integration we get

$$F_1 = \ln\frac{P_t - P_\infty}{P_0 - P_\infty} = -k_1 t \tag{4}$$

$$F_2 = (P_0 - P_\infty)\ln\frac{P_0 - P_\infty}{P_t - P_\infty} - (P_0 - P_t) = \frac{1}{2}k_2 t \tag{5}$$

for the rate law 2 and 3, respectively.

Analysis of kinetic data from several runs at each reaction temperature adopted in KIE determination were performed. All

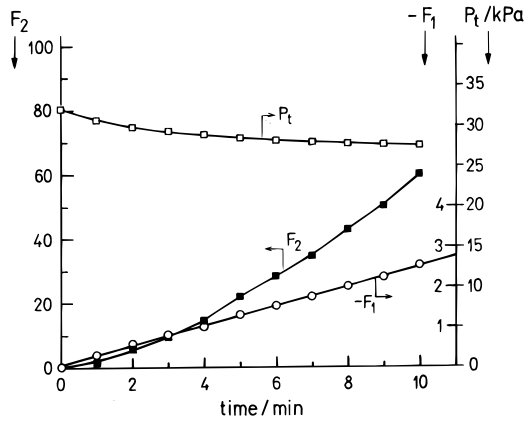

Figure 1. Test plots of integrated rate laws for the silver catalyzed carbon monoxide oxidation at 373 K: □, P_t, total pressure time course (kPa); ○, eq 4; ■, eq 5; catalyst mass, 3 g of silver wool; starting mixture $CO:O_2 = 1:2$.

TABLE 2: Normalized Rate Constants k_n (eq 6) for the Silver-Catalyzed Carbon Monoxide Oxidation (from Four Runs for Each Temperature)

temp, K	323	373	413	453
1000 k_n, $m^2\ s^{-3}$	1.10 ± 0.05	5.6 ± 0.3	42 ± 2	152 ± 7

the experimental data were fitted by eqs 4 and 5. With eq 5 a marked deviation from linearity was found, while with eq 4 linear plots appeared. Figure 1 shows typical plots for a representative run at 373 K using eqs 4 and 5 versus time. Thus, we may conclude that, under our reaction conditions, the oxidation obeys the rate law $dP_{CO}/dt = -k_1 P_{CO}$, i.e., it is of the order of +1 with respect to carbon monoxide pressure and order of 0 with respect to oxygen and carbon dioxide pressure.

Activation Energy. To determine the activation energy the oxidations were conducted at 343 and 373 K with 3 g and at 413 and 453 K with 0.12 g of the same silver catalyst. In addition, results from the kinetic isotope effects measurements were applied to calculate rate constants. To use the data from the kinetics and KIE experiments the overall rate constants were expressed in the form

$$k = k_n \frac{m}{V} \tag{6}$$

where k_n is the rate constant normalized to the mass of catalyst, m, and the reaction volume, V. Rate constants, k_n, from subsequent runs conducted on stabilized (conditioned) catalyst, were reproducible within 10%, in general. The averaged values for the above reaction temperatures (4 runs for each temperature) are given in Table 2. The Arrhenius plot of ln k_n vs $1/T$ (given in Figure 2) yields an apparent activation energy of 59.3 ± 1.7 kJ mol^{-1}.

4. Discussion

Theoretical interpretation of the experimental kinetic isotope effects was made following Bigeleisen's formalism based on the absolute rate theory. The carbon-13 kinetic isotope effects may accordingly be calculated from the equation[30]

$$\frac{k_{12}}{k_{13}} = \frac{\nu^{\neq}_{L,12}}{\nu^{\neq}_{L,13}} \prod_{i=1}^{3n-6} \frac{u_{13,i}}{u_{12,i}} \frac{\sinh(u_{12,i}/2)}{\sinh(u_{13,i}/2)} \prod_{i=1}^{3n^{\neq}-7} \frac{u^{\neq}_{12,i}\sinh(u^{\neq}_{13,i}/2)}{u^{\neq}_{13,i}\sinh(u^{\neq}_{12,i}/2)}$$

in which $^{\neq}$ denotes the transition state. The first product runs over all the isotopic frequencies of the reactant molecules and

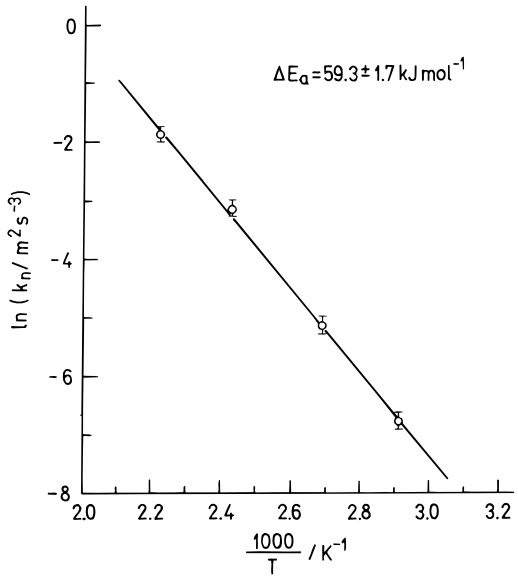

Figure 2. Arrhenius plot of ln k_n vs.1/T.

the second over the real frequencies of the transition state; ν_L is the frequency belonging to the reaction coordinate; $u_i = hc\omega_i/k_BT$ (ω_i, wavenumber of the i-th normal vibration in cm^{-1}; h, Planck's constant; k_B, Boltzmann's constant; c, speed of light; T, temperature).

The isotopic normal frequencies for the reactant CO molecule were obtained from the literature,[31] while those for the transition state by solving Wilson's FG matrix equation[32−34]

$$\mathbf{GFL} = \mathbf{L\Lambda}$$

in which **G** is the Wilson matrix, **F** is the force-constant matrix, **L** is the eigenvector matrix, and Λ is a diagonal matrix of eigenvalues $\lambda_{ii} = 4\pi^2\nu_i^2$ with ν_i equal to the frequency of the i-th normal vibration.

As transition states, $(CO_2)^{\ddagger}$ of different geometries and force constants were checked. For the internal coordinates, changes of both C−O bond lengths, designated by D and d, and of the interbond angle α were taken. In calculations, the values of diagonal **F** matrix elements were varied in the following ranges: F_D and F_d from 100 to 2000 N m^{-1} with steps of 100 N m^{-1}, F_α from 50 to 300 N m^{-1} in steps of 50 N m^{-1} (100 N m^{-1} equals 1 mdyn $Å^{-1}$). The interbond angle α took values between 80 and 170° in 10° steps. The off-diagonal elements were set at zero, with the only exception of the F_{Dd} element needed to get a zero determinant of the **F** matrix thus resulting in one zero normal frequency belonging to the reaction coordinate. Its value was calculated from the equation $F_{Dd} = \pm(F_DF_d)^{1/2}$.

In our case only an asymmetric stretching vibrational normal mode ("+" at the above square root) of the transition state can describe the movement along the reaction coordinate—CO_2 formation: one of the bonds is weakened from its value in the adsorbed CO (2000 N m^{-1}) to a value in CO_2 (1600 N m^{-1}),[35,36] while the other bond is formed, thus having a stretching force constant between zero and a value in CO_2. Among various force constant (F) and bond length (r) relations for CO molecule,[36] the empirical formula $F = 35.5/r^{5.79}$ was chosen.[37] An agreement between the calculated and experimental kinetic isotope effects was sought by a graphic method already used elsewhere in which, for selected values of other parameters of the transition state, a region of acceptable values of both streching force constants is obtained.[37]

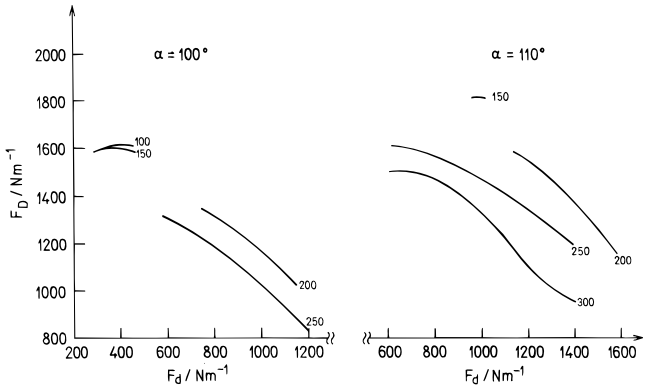

Figure 3. Ranges of acceptable values of both stretching force constants for selected values of the bending force constant, F_α (numbers attached to curves, N m^{-1}), and interbond angles of 100° and 110°.

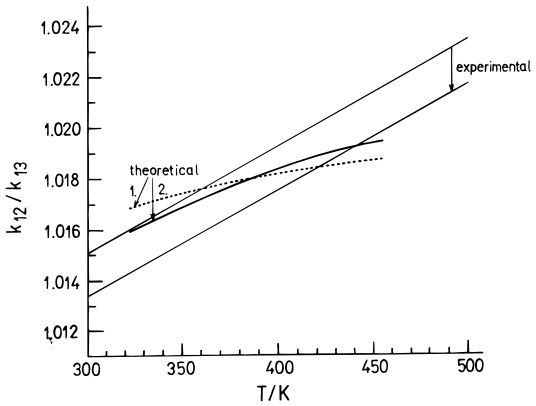

Figure 4. Agreement with the experiment for two examples of the $(CO_2)^{\ddagger}$ transition state with parameter values listed under (1) and (2) in Table 3.

In Figure 3 the acceptable ranges of values of force constants are shown for interbond angles of 100° and 110°. Values of interbond angles below and above do not give agreement with the experiment. They fail with respect to their temperature dependence. Thus, for example, for α = 120° and F_D = 1800 N m^{-1}, the acceptable values for F_d are 200−290 N m^{-1} at 473 K and 50−100 N m^{-1} at 323 K; they do not match. We describe the reaction coordinate by the asymmetric normal mode of the transition state in which one of the bonds has a force constant between the value in CO and CO_2 (weakening of the previously existing C−O bond), while the value of the force constant of the other bond is below the value in CO_2 (a new C−O is being formed). We are thus interested in those $(CO_2)^{\ddagger}$ transition states with one C−O bond of 1600−1800 N m^{-1} and the other of 0−1600 N m^{-1}. For α = 100° these ranges of values attract our attention: if F_D = 1600 N m^{-1}, then F_d may take values in the range of 350−450 and 300−450 N m^{-1} for F_α = 100 and 150 N m^{-1}, respectively. Among ranges for 110°, we may pick up only F_D = 1800 N m^{-1}, F_d = 1000−1050 N m^{-1}, F_α = 150 N m^{-1}, and F_D = 1600 N m^{-1}, F_d = 1100 N m^{-1}, F_α= 200 N m^{-1}, the remaining values do not fit our requirements. In Figure 4, agreement with the experiment is shown for two transition states for which the parameters are listed in Table 3. Angle 110° is more favorable.

Conclusions

In our theoretical interpretation of the ^{13}C kinetic isotope effects in the CO oxidation over Ag surface, we applied $(CO_2)^{\ddagger}$ transition states with various geometries. The experimental values were satisfactorily reproduced by a bent $(CO_2)^{\ddagger}$ transition

TABLE 3: Geometries, Force Constants, and Isotopic Frequencies of Normal Vibrations of Two Successful Examples of the $(CO_2)^{\ddagger}$ Transition State[a]

	F_D, N m^{-1}	F_d, N m^{-1}	F_α, N m^{-1}	D, pm	d, pm	ω_{12}, cm^{-1}	ω_{13}, cm^{-1}
(1) $\alpha = 100°$	1600	450	120	115	143	2185.3	2138.2
						540.2	534.3
						0	0
(2) $\alpha = 110°$	1600	1100	200	115	122	2383.3	2335.2
						753.0	746.3
						0	0

[a] In each case first frequency corresponds to the symmetric stretching vibration, second frequency to the bending vibration, and third zero frequency corresponds to the asymmetric stretching vibration−decomposition mode.

state with the asymmetric normal mode as the reaction coordinate. The interbond angle is close to 110° and values of stretching force constants are in ranges of 1600−1800 and 1000−1050 N m^{-1}. This confirms the assumption that in the rate determining step a CO molecule reacts with only one adsorbed oxygen atom as suggested from other studies and gives numerical values at the geometrical parameters and the vibrational frequences of the transition state in this step.

Acknowledgment. U. Burghaus acknowledges financial support from the Deutsche Forschungsgemeinschaft. The research was financially supported by the Slovene Ministry of Science and Technology.

References and Notes

(1) Ertl, G.; Rau, P. *Surf. Sci.* **1969**, *15*, 443.
(2) Engel, T.; Ertl, G. *Adv. Catal.* **1979**, *28*, 2 and references therein.
(3) Stampfl, C.; Scheffler, M. *Phys. Rev. Lett.* **1997**, *78*, 1500; *Surf. Sci.* **1997**, *377/379*, 808. Kang, H. C.; Jachimowski, T. A.; Weinberg, W. H. *J. Chem. Phys.* **1990**, *93*, 1418.
(4) Taylor K. C. *Catal. Rev.* **1993,** *35*, 457 and references therein.
(5) Gardner, S. D.; Hoflund, G. H.; Schryer, D. R.; Schryer, J.; Upchurch, B. P.; Kielin, E. J. *Langmuir* **1991**, *7*, 2135.
(6) Burghaus, U.; Conrad, H. *Surf. Sci*. **1995**, *338*, L869; *Surf. Sci*. **1997**, *370*, 17.
(7) Burghaus, U.; Conrad, H. *Surf. Sci.* **1996**, *352*−*354*, 201.
(8) E.g.: Bowker, M.; Guo, Q.; Joyner, R. W. *Surf. Sci.* **1991**, *253*, 33. Bowker, M.; Guo, Q.; Joyner, R. W. *Surf. Sci.* **1993**, *280*, 50. Surnev, L.; Bliznakov, G.; Kiskinova, M. *Surf. Sci.* **1984**, *140*, 249. Milun, M.; Pervan, P.; Vajic, M. *Surf. Sci.* **1989,** *211/212*, 887. Sasaki, T.; Sueyoshi, T.; Iwasawa, Y. *Surf. Sci.* **1994**, *316*, L1087. Taylor, J. L.; Ibbotson, D. E.; Weinberg, W. H. *Surf. Sci.* **1979**, *90*, 37; *J. Chem. Phys.* **1978**, *69*, 4298. Zhdanov, V. P. *Surf. Sci.* **1984**, *137*, 515; *Surf. Sci.* **1982**, *123*, 106. Burghaus, U.; Ding, J.; Weinberg, J. W. *Surf. Sci.* in press.
(9) E.g.: Keulks, G. W.; Chang, C. C. *J. Phys. Chem.* **1970**, *74*, 2590.
(10) Cf.: de Mongeot, F. B.; Valbusa, U.; Rocca, M. *Surf. Sci.* **1995**, *339*, 291.
(11) E.g.: McElhiney, G.; Papp, H.; Pritchard, J. *Surf. Sci.* **1976**, *54*, 617. Peterson L. D.; Kevan, S. D. *J. Chem. Phys.* **1991**, *95*, 8592. Burghaus, U.; Conrad, H. *Surf. Sci*. **1995**, *331*−*333*, 116.
(12) Burghaus, U.; Vattuone, L.; Gambardella, P.; Rocca, M. *Surf. Sci*. **1997**, *374*, 1.
(13) E.g.: Matsushima, T. *Surf. Sci.* **1983**, *127*, 403. Mieher W. D.; Ho, W. *J. Chem. Phys.* **1989**, *91*, 2755; *J. Chem. Phys.* **1989**, *99*, 9279.
(14) Capote, A. J.; Roberts, J. T.; Madix, R. J. *Surf. Sci*. **1989**, *209*, L151. Burghaus, U.; Conrad, H. *Surf. Sci*. **1996**, *352*−*354*, 253; *Surf. Sci*. **1996**, *364*, 109.
(15) Koel, B. *ACS Symposium*; Oyama, Hightower, Eds.; *Su. 523*, **1993**, and private communications.
(16) Brown, L. S.; Sibener, S. J. *J. Chem. Phys.* **1989**, *90* (5), 2807.
(17) Campbell, C. T.; Ertl, G.; Kuipers, H.; Segner, J. *J. Chem. Phys.* **1980**, *73* (11), 5862.
(18) Allers, K. H.; Pfnür, H.; Feulner, P.; Menzel, D. *J. Chem. Phys.* **1994**, *100*, 3985.
(19) Michael, J. V.;. *J. Chem. Phys.* **1989**, *90* (1), 189.
(20) Reijnen, P. H. F.; Raukema, A.; van Slooten, U.; Kleyn, A. W. *J. Chem. Phys.* **1991**, *94* (3), 2368.
(21) Reijnen, P. H. F.; Raukema, A.; van Slooten, U.; Kleyn, A. W. *Surf. Sci.* **1991**, *253*, 24.
(22) Tanner, M. J.; Brookhart, M.; DeSimone, J. M. *J. Am. Chem. Soc.* **1997**, *119*, 7617.
(23) Zielinski, M.; Papiernik- Zielinska, H.; Zielinska, A.; Kasprzyk, G.; Czarnota, G.; Städter, W.; Gehre M. *J. Radioanal. Nucl. Chem., Articles* **1996**, *210*, 15.
(24) Zielinski, M.; Zielinska, A.; Bernasconi S.; Papiernik- Zielinska, H. *J. Radioanal. Nucl. Chem., Articles* **1997**, *220*, 263.
(25) Lesar, A.; Senegačnik, M. *J. Chem. Phys.* **1993,** *99*, 187.
(26) Bigeleisen, J.; Wolfsberg, M. *Advances Chem. Phys.* **1958**, *1*, 15.
(27) Senegačnik, M. *Ph.D. Thesis*, Université de Paris, 1957, CEA (Commissariat à lEnergie Atomique), Report CEA-R-726, 1957.
(28) Kobal, I.; Senegačnik, M.; Kobal H. *J. Catal.* **1977**, *49*, 1.
(29) Ogrinc, N.; Kobal, I.; Senegačnik, M. *J. Phys. Chem.* **1997**, *101*, 7236.
(30) Van Hook, W. A. *Isotope Effects in Chemical Reaction;* Van Nostrand-Reinhold: New York, 1970.
(31) Nakamoto, K. *Infrared Spectra of Inorganic and Coordination Compounds*; Wiley: NewYork, 1963.
(32) Wilson, E. B.; Decius, J. C.; Cross, P. C. *Molecular Vibrations*; McGraw-Hill: New York, 1965.
(33) Guns, P. *Vibrating Molecules*; Chapman & Hall: London, 1971.
(34) Barliè, B. *MS Thesis*, University of Ljubljana, 1973.
(35) Herzberg, G. *Molecular Spectra and Molecular Structure II, Infrared and Raman Spectra of Polyatomic Molecules*; Van Nostrand: New York, 1949.
(36) Goldman, A. S.; Krog-Jespersen, K. *J. Am. Chem. Soc.* **1996**, *118*, 12159.
(37) Ladd, I. A.; Orville-Thomas, W. J.; Coc, B. C. *Spectrochim. Acta* **1964**, *20*, 1977.